

Published in final edited form as:

Nat Electron. 2019 December ; 2(12): 606–611. doi:10.1038/s41928-019-0333-z.

Touchscreen tags based on thin-film electronics for the Internet of Everything

Nikolaos Papadopoulos¹, Weiming Qiu¹, Marc Ameys¹, Steve Smout¹, Myriam Willegems¹, Filip Deroo⁴, Jan-Laurens van der Steen², Auke Jisk Kronemeijer², Marco Dehouwer³, Alexander Mityashin¹, Robert Gehlhaar¹, Kris Myny¹

¹imec, Large Area Electronics, Leuven, 3001, Belgium ²TNO/Holst Centre, Eindhoven, 5605, Netherlands ³Cartamundi, Turnhout, 2300, Belgium ⁴Cartamundi Digital, Drongen, 9031, Belgium

Abstract

Capacitive touchscreens are increasingly widespread, featuring in mobile phones and tablets, as well as everyday objects such as cars and home appliances. As a result, the interfaces are uniquely placed to provide a means of communication in the era of the Internet of Everything. Here we show that commercial touchscreens can be used as reader interfaces for capacitive coupled data transfer. The transfer of data to the touchscreen is achieved using a 12-bit thin-film capacitive radio frequency identification tag powered by a thin-film battery or a thin-film photovoltaic cell that converts light from the screen. The thin-film integrated circuit has a 0.8 cm² on-chip monolithic antenna, employs 439 transistors, and dissipates only 31 nW of power at a supply voltage of 600 mV. The chip has an asynchronous data rate of up to 36 bps, which is limited by the touchscreen readout electronics.

In the Internet of Things (IoT), millions of devices are connected to cloud-based services by means of different wireless communication protocols – including WiFi, Bluetooth Low Energy, and 4G/5G – embedded on one or several silicon complementary metal–oxide–semiconductor (CMOS) chips. To enable the transition from IoT to Internet of Everything (IoE), everyday items need to be equipped with wireless communication chips that are low-cost and seamlessly integrated. Thin-film transistor (TFT) technology on plastic substrates is a promising candidate to provide these IoE communication functions. The technology can, in particular, provide flexible radio-frequency identification (RFID) tags^{1,2,3,4,5,6,7,8,9} that can be concealed in numerous different objects such as paper tickets, official letters, certified documents, and payment cards.

Users may view, print, copy, and download text and data-mine the content in such documents, for the purposes of academic research, subject always to the full Conditions of use:http://www.nature.com/authors/editorial_policies/license.html#terms

Author contributions statement

N.P. and K.M. conceived conducted and analyzed the experiment(s), M.A. conceived experiments, R.G. and W.Q. conducted the TFPV analysis and fabrication, F.P. developed the apps, S.S. and M.W. A.K and J-L.S conducted the fabrication, M.D. and A.M. conceived the applications. All authors reviewed the manuscript.

Data availability

The data that support the plots within this paper and other findings of this study are available from the corresponding author upon reasonable request.

In proposed implementations of the IoE, a device/reader serves as a hub that connects everyday items and objects via short-range communication (RFID) to the cloud. One initial potential scenario uses a TFT-based near-field communication (NFC) chip^{5,7,10}, as many people have access to phones and tablets equipped with an accessible NFC reader. However, the number of connected NFC-enabled devices is still relatively small, compared to the wide availability of touchscreens – and thus, with the right communication technology, touchscreens could play a key role in delivering the IoE¹¹.

Although initially unforeseen¹², a capacitive touchscreen can now be considered as a data communication medium for objects equipped with an identification chip. Data transfer occurs via the capacitive antennas present on the chip and touchscreen. Capacitive communication offers many advantages, including security (due to the very short communication range¹³), low cost (due to the possibility of monolithically integrating antennas, no need for assembly and extra antenna substrate) and widespread compatibility (due to the presence of capacitive touchscreens in everyday devices such as cars, refrigerators, and coffee machines).

Novel forms of touchscreen interaction have already been demonstrated by combining Si-CMOS chips and non-conventional off-the-shelf components such as bipolar transistors, mechanical relays, and tri-state buffers^{13,14,15,16}. Such non-conventional components are selected for their high off-state resistance required to virtually switch off a touch event, mimicking to release a finger from the screen, limiting the potential for a monolithic low-cost Si-CMOS solution. Metal-oxide TFT technologies exhibit a very low off-current leakage²⁰, which can be translated into a substantially high off-resistance interface to the screen. In addition, the technology uses a self-aligned transistor architecture that has minimal capacitance and could provide a monolithic solution for touchscreen communication.

We recently reported monolithically-integrated capacitive coupled thin-film RFIDs that used a custom-built reader^{2,3}. In this Article, we report a TFT-based chip that can communicate electrically with commercial capacitive touchscreens. Our chip is a capacitive RFID tag made from indium gallium zinc oxide (IGZO) thin-film transistor technology on plastic substrates. It can be powered by a thin-film battery that provides a continuous 1.5 V or thin-film photovoltaic cell that can generate up to 600 mV from the incident light of a smartphone display. The tag system and communication method are tested using a range of different touchscreens from a variety of brands, including Apple, Samsung, and Huawei.

TFT fabrication and electrical characterization

A self-aligned TFT architecture on a GEN1 (350mmx320mm) plastic substrate¹⁷ is used to fabricate the Capacitive-touchscreen-tags (C-touch) tags (Fig. 1). Using a temporary glass carrier with a 15- μm -thick polyimide film, a humidity barrier is deposited. Next, a thin layer IGZO is DC sputtered and patterned to define the active semiconductor area. Then, to create a gate dielectric, a 200-nm-thick layer of SiO₂ is deposited using plasma-enhanced chemical vapour deposition (PECVD) at a temperature of 250°C. Afterwards, 130-nm-thick MoCr is added as gate-metal. The dielectric and gate metal area is defined by subsequent etching

steps during the same photolitho-step. Next, 200-nm-thick SiNx is deposited using PECVD in order to act as intermetal dielectric and so that hydrogen dopes the IGZO (decreasing its resistance) in the areas not covered by the SiO₂ gate dielectric. The contact holes for the source-drain (SD) contacts are opened and MoCr/Al/MoCr is deposited and patterned to define the SD contacts. The stack is passivated by a thick (around 2 μm) organic photo-exposable and curable interlayer/pixel definition layer material from Tokyo Ohka Kogyo Co Ltd and 130-nm-thick MoCr is deposited and patterned. The last step in the TFT process is a final anneal at 165°C. All process steps in the backplane process stay below a thermal budget of 350°C.

The transfer characteristics and gate current of 24 TFTs with a width/length of 20 μm/40 μm are shown in Fig. 1b. The measurements have been obtained on various locations across the 150 mm² plate. The 20/40 TFT is one most commonly used in our design and one of the smallest TFTs in the circuit blocks. The extracted average charge carrier mobility and threshold voltage distributions are shown in Fig. 2c,d. The median threshold voltage (V_T) is 0.65 V and the median mobility (μ) is 10.7 cm²/Vs. Moreover, the standard deviation of V_T is only 34 mV, the standard deviation of μ is 0.28 cm²/Vs across 150mm² on the plate. Self-aligned TFTs have negligible parasitic capacitance between gate and source-drain contacts, and have been shown to be compatible with capacitive RFIDs^{2,3}. Furthermore, modifying the thickness of gate dielectric improves the input capacitance of the TFT: it results in 9 pF for a 50 nm thick gate dielectric, 6 pF for a 100 nm thick dielectric and 4 pF for a 200 nm thick dielectric for a 1500 μm /5 μm TFT. This is an important parameter for enabling communication to a capacitive touchscreen.

Thin-film photovoltaic fabrication and characterization

Our thin-film photovoltaic (TFPV) has the following structure: glass/indium tin oxide (ITO)/poly [N, N'-bis(4-butylphenyl)-N,N'-bis(phenyl)-benzidine] (PolyTPD)/perovskite/Phenyl-C61-butyric acid methyl ester (PCBM)/ZnO/Al (Fig. 2a), where the nominal composition (calculated from the precursor solution) of the perovskite is Cs_{0.1}FA_{0.9}Pb_{2.865}Br_{0.135}, whereby FA refers to formamidinium. The average power conversion efficiency (PCE) after encapsulation is 13.5% ± 0.5%. A typical current density-voltage (J-V) curve is shown in Fig. 2b, exhibiting a short-circuit current (J_{sc}) of 19.1 mA/cm², an open-circuit voltage of 0.97V, and a fill factor of 76% under AM 1.5G spectrum. This device gives a steady PCE of 13.7% when operating at 0.79V, which is maximum power point obtained from the J-V scan (inset of Fig. 2b). The fabrication process is also compatible with flexible substrates^{18,19}, offering monolithic integration possibilities for the C-touch tag. A photo of the cells is shown in Fig. 5d.

The I-V curve and power output of one individual photovoltaic cell with 12.5 mm² active area placed on a white colour screen of a Samsung Galaxy S8 phone is shown in Fig. 2c,d. Screen brightness is varied in three levels (25%, 50% and 100%) and the voltage is swept from 0.9 V to -0.1 V and back with a delay time of 0.02s between each measurement point. For 25% screen brightness the maximum achieved power is ~400nW at 600 mV. As expected, increasing the brightness of the screen increases the harvested power from the

photovoltaic, achieving $7\mu\text{W}$ at 100% brightness (as indicated by the phone). The phone was not fully charged to emulate an average use case.

System design consideration

The detailed schematic of the flexible C-touch tag, and a typical illustration of a touchscreen and its electronics, is shown in Fig. 3a. The physical structure of the interface between the touchscreen and the C-touch tag together with its main blocks is shown in Fig. 3b. The touchscreen's transparent metal lines are considered as the bottom plate of the capacitive coupler and the electrodes of the tag serve as top plates. The glass of the touchscreen combined to the plastic or paper of the tag forms the dielectric of the capacitive coupler. The roughness of different materials (glass/paper/plastic) adds air to the dielectric mix, impeding the coupling of the tag to the touchscreen.

The complexity and diversity of modern touchscreens^{20,21} and their electronics^{22,23,24,25,26} is not captured in Fig. 3; it focuses instead on the interface between the tag and the touchscreen and illustrates its main properties. The power block of the TFT tag can be either a thin-film battery (TFB) or a thin-film photovoltaic cell (TFPV). TFBs are available from 1.5 V to 4 V. Open circuit voltage of TFPVs have recently improved reaching 0.8 V^{27,28} for organic cells, or around 1.2 V for perovskite solar cells²⁹. The creation of higher voltages using only TFPVs requires expensive and complicated fabrication methods to connect TFPV cells in series forming a module. Another option would be to implement a DC-DC up-converter to generate larger voltage levels. However, the high brightness of modern displays ($>550\text{ cd/cm}^2$) is enough to power the C-touch tag at 600 mV (illustrated in Fig. 3), offering a monolithic solution for the full C-touch system.

The main blocks of the flexible integrated circuit are a clock generator, a 12-bit code generator, a modulator and the electrodes. The TFT sizing of the various block of the tag is shown in Fig. 4b. The clock generator is a very critical block because it controls the data transmission rate to the touchscreen. Experiments indicate that the touch event readout rate (sampling rate S/s) is limited to only 60 events/sec. These sets of experiments (Fig. 4e) were performed on multiple touchscreens using various electrode sizes, a discrete off-the-shelf-components built lab emulator (seen in Fig. 4f), and a special touch event app. The same speed is confirmed by swiping a human-finger on a touchscreen using the same touch event extraction app, setting a clock speed specification (Hz) to the clock generator as seen in Fig. 4c. To meet the slow speed challenge the channel length of the 19-stage ring oscillator (RO), used as a clock generator, is selected to be 200 μm and 400 μm , whereby a capacitor is included at the output of the RO for both battery and PV power source. The 200 μm channel length design is selected because at 600 mV the speed of the 400 μm length is impractically slow (2.8 Hz). The power of the 200 μm RO measures 7.7 nW at 600 mV.

The 12-bit code generator (CG) with hard-wired memory embedding a bit-sequence *0101 0011 0110* is designed using pseudo-CMOS logic gates³⁰ with single supply operation^{2,3} employing 439 transistors. The channel length of the logic gates is selected to be 40 μm (Fig. 4b) to reduce total power dissipation of the tag to prolong its lifetime in case of battery use or to reduce the footprint of the PV cell. A typical commercially available TFB (0.5 mm

thick) is providing 1.5 mAh/cm² power at 3 V³¹. The CG is dissipating ~10 μW at 3 V yielding approximately 450 hours of continuous operation using a 1 cm² TFB. Lowering the power supply to 1 V multiplies the lifetime of the tag with more than an order of magnitude. At 600 mV the CG dissipates less than 23 nW power, which results to total chip power dissipation of ~31 nW, leading to more than 9.5 years of continuous operation using a TFB. In addition, this low power value would enable a monolithic solution whereby a TFPV can be directly integrated on top of a TFIC, requiring minimum footprint. Figures 4c,d indicate that RO and CG are operational at 600 mV and prove that no serial connection of multiple TFPV cells nor a DC-DC converter circuit is necessary.

The modulator of the tag is a large-sized TFT connected to the output of the CG after a 2-stage buffer enhancing rise and fall times of the signal. The large W/L (1500/10) is selected to improve the modulation and the distinction between a digital 0 and 1. Therefore, it facilitates the identification of the code from the touchscreen and the application running on the device.

As mentioned earlier, the sizes of the electrodes have been evaluated using a developed lab touch emulator (Fig. 4f). In Fig. 4e the need for 8x5 mm² electrodes is illustrated to achieve 24 bps data rates. Many different devices (iPad, iPhone SE, iPhone 8, Samsung S4, S8 and Note8, and Huawei Y7) were tested using 1x1, 2x2, 5x5 and 5x8 (mm x mm) electrodes. Figure 4e indicates that larger-sized electrodes achieve a better data transmission rate and improve the readout of the modulation of the tag at the touchscreen. The mm-range size of the electrodes defines the size of the tag and provides large-area thin-film electronics an important advantage compared to standard silicon CMOS technologies. Two electrodes are used in the developed algorithm, whereby one electrode is permanently connected to ground, and the other is connected to/disconnected from the ground depending on the bit-sequence *0101 0011 0110*. A '1' is creating a swipe event on the touchscreen from the permanently grounded electrode to the other.

C-touch tag experiments

Figure 5a shows the setup used to connect the flexible TFT C-touch tag (with 0.8 cm² electrodes) to a commercially available flexible battery and Fig. 5d the C-touch tag connected to the developed TFPV. The interconnection PCB is only present to make the physical connection of the two parts, no additional electronics are present on the PCB. All the circuitry of Fig. 4 is integrated on the TFT C-touch tag. The orange horizontal and vertical lines on the touchscreen are crossing at the precise point of the generated touch event and are visible in Fig. 5. In Fig. 5c a zoom-in to the delaminated flexible C-touch tag without rigid support carrier is shown, indicating the different circuit blocks.

Fig.6 shows the extracted touch event relocation data ($DY=Y-Y_0$) as obtained from 3 commercial phones without any change in their hardware or firmware settings. Y_0 is the pixel's y-axis coordinate of the first touch event and Y the coordinate for the specific time. In Fig. 6a,b the DY data were received from experiments where the C-touch tag was driven by 1.5 V TFB, as shown in Fig. 6a,b. In Fig.6 (a) the actual and 12-bit code sequence is indicatively illustrated with a blue dotted line to assist the understanding of the DY data. The

hard-wired bit-sequence of the flexible tag can be detected by using the prediscussed touchscreen communication protocol. The 2 phones achieve similar transmission rates of 17-19bps but differ in maximum relocation of the touch event (DY_{max}). The DY_{max} strongly depends on the resolution of the display and the touchscreen readout chip. By comparing the plots in Fig.6, it can be concluded that the sampling rates (pink dots) of the touchscreen electronics are not similar for all phones. The same behaviour is shown in Fig. 4e, where similar experiments were performed using the lab C-touch emulator.

In a subsequent step, a gamecard paper (170 μm thick) and a typical plastic screen protector have been placed in between the tag and the touchscreens, as indicated in Fig. 6b (for the paper case). No differences were observed either to the relocation DY or the speed of the data transmission rate to the touchscreen.

In Fig. 6c a faster data rate is achieved by driving the TFT C-touch tag at a higher supply voltage (2.2 V). The obtained relocation data are a bit less clear compared to Fig. 6d, but still more clear compared to other phones. Similar experiments of increasing data rates were performed on other phones as well, whereby the bit-sequence was not always detectable. This implies that with the current state of touchscreen technology, a universal upper limit in data rate should be used to ensure compatibility to a wide range of phones. Obviously, one method to increase data rates with the proposed C-touch tags would be a multitouch-multi-swipe event, whereby multiple electrodes can serve as input node. Another method was proposed earlier in the literature¹³ by modifying the firmware of the touchscreens readout hardware, obtaining up to 500 kb/s data transfer, paving the way for more complex data communication to touchscreens, enabling a broader variety of applications.

Figure 6d plots the captured data by the touchscreen whereby the C-touch tag is powered by the TFPV. The circuit and TFPV are connected by the same interconnect PCB and wiring as for the TFBAT. The PV cell and tag have been placed on the smartphone display as shown in Fig. 5d. The brightness of the display of the smartphone was regulated so that 610 mV is achieved by the TFPV. The tag achieves correct transmission of 12-bit code to the touchscreen. The slow speed of 4 bps is due to the ring oscillator integrated on the tag. Faster speeds can be achieved, integrating a faster ring oscillator as shown from Fig. 4c.

Conclusions

We have reported capacitive coupled data transfer using a flexible C-touch chip (a capacitive RFID tag) based on thin-film transistor technologies and commercial touchscreens as a reader interface. The tag can be integrated with a thin-film battery that provides a continuous 1.5 V. Alternatively, it can be connected to a thin-film, foil-compatible photovoltaic cell that has an active area of only 12.5 mm^2 ; the photovoltaic cell can generate 600 mV from the incident light of a smartphone display. The C-touch tag can achieve data transfer rates of up to 36 bps at a supply voltage of 2.2 V provided by external power supply or battery. This is in the range of detectable sampling rates of current pristine touchscreen readout electronics. The power consumption of the tag was four times lower than the previously reported 12-bit code generator² and dissipated only 31 nW at a 600 mV supply. Our C-touch tag technology could potentially be implemented on 4.5 billion mobile phones worldwide and the extra

touchscreen-enabled devices (cars, home appliances, smart surfaces, tables) in the near future without additional costs for the users.

Acknowledgements

The authors would like to thank the process engineers of Holst Centre's GEN1 Pilot Line for fabricating the circuits presented in this paper. This work has received funding from the European Research Council (ERC) under the European Union's Horizon 2020 research and innovation program under grant agreement No 732389 (CAPID project) and No 716426 (FLICs project). Part of this work is financed through the Flexlines project within the Interreg V-programme Flanders-The Netherlands, a cross-border cooperation programme with financial support from the European Regional Development Fund, and co-financed by the Province of Noord-Brabant, The Netherlands. W. Q. would like to thank the financial support of the postdoctoral researcher grant (12Z4618N) received from Research Foundation Flanders (FWO), Belgium.

References

1. Cantatore E, et al. A 13.56-MHz RFID System Based on Organic Transponders. *IEEE J Solid-State Circuits*. 2007; 42:84–92.
2. Papadopoulos N, et al. 2-D Smart Surface Object Localization by Flexible 160-nW Monolithic Capacitively Coupled 12-b Identification Tags Based on Metal-Oxide TFTs. *IEEE Trans Electron Devices*. 2018:1–7.
3. Papadopoulos, N; , et al. 1cm²sub-1V Capacitive-Coupled Thin Film ID-Tag using Metal-oxide TFTs on Flexible Substrate. 2018 International Flexible Electronics Technology Conference (IFETC); 2018. 1–2.
4. Hung, M-H; , et al. Ultra Low Voltage I-V RFID Tag Implement in a-IGZO TFT Technology on Plastic. *IEEE Int Conf RFID 5*; 2017.
5. Myny K. The development of flexible integrated circuits based on thin-film transistors. *Nat Electron*. 2018; 1:30–39.
6. Yang B-D. A Transparent Logic Circuit for RFID Tag in a-IGZO TFT Technology. *ETRI J*. 2013; 35:610–616.
7. Myny K, Tripathi AK, van der Steen J-L, Cobb B. Flexible thin-film NFC tags. *IEEE Commun Mag*. 2015; 53:182–189.
8. Klauk H, Zschieschang U, Pflaum J, Halik M. Ultralow-power organic complementary circuits. *Nature*. 2007; 445:745–748. [PubMed: 17301788]
9. Ke T-H, et al. Scaling down of organic complementary logic gates for compact logic on foil. *Org Electron*. 2014; 15:1229–1234.
10. Myny, K; , et al. 15.2 A flexible ISO14443-A compliant 7.5mW 128b metal-oxide NFC barcode tag with direct clock division circuit from 13.56MHz carrier. 2017 IEEE International Solid-State Circuits Conference (ISSCC); IEEE; 2017. 258–259.
11. Villar, N; , et al. Project Zanzibar: A Portable and Flexible Tangible Interaction Platform. *Proceedings of the 2018 CHI Conference on Human Factors in Computing Systems - CHI '18*; ACM Press; 2018. 1–13. doi:10/gfsjqx
12. Johnson EA. Touch Displays: A Programmed Man-Machine Interface. *Ergonomics*. 1967; 10:271–277.
13. Vu T, et al. Capacitive Touch Communication: A Technique to Input Data through Devices' Touch Screen. *IEEE Trans Mob Comput*. 2014; 13:4–19.
14. Coni P, Perbet J-N, Augros L, Abadie JC, Sontag Y. 6.1: A New Application of a Touch Screen Display for Data Transfer. *SID Symp Dig Tech Pap*. 2015; 46:37–40.
15. Yu, N-H; , et al. TUIC: enabling tangible interaction on capacitive multi-touch displays. *Proceedings of the 2011 annual conference on Human factors in computing systems - CHI '11*; ACM Press; 2011. 2995doi:10/cpm7js
16. Kubitzka, T; Pohl, N; Dingler, T; Schmidt, A. WebClip: a connector for ubiquitous physical input and output for touch screen devices. *Proceedings of the 2013 ACM international joint conference on Pervasive and ubiquitous computing - UbiComp '13*; ACM Press; 2013. 387doi:10/gfsjqz

17. Kronemeijer AJ, et al. P-127: Dual-Gate Self-Aligned IGZO TFTs Monolithically Integrated with High-Temperature Bottom Moisture Barrier for Flexible AMOLED. SID Symp Dig Tech Pap. 2018; 49:1577–1580.
18. Qiu W, et al. High efficiency perovskite solar cells using a PCBM/ZnO double electron transport layer and a short air-aging step. *Org Electron*. 2015; 26:30–35.
19. Qiu W, et al. An Interdiffusion Method for Highly Performing Cesium/Formamidinium Double Cation Perovskites. *Adv Funct Mater*. 2017; 27
20. Xiao F, Wang Z, Ye N, Wang R, Li X-Y. One More Tag Enables Fine-Grained RFID Localization and Tracking. *IEEEACM Trans Netw*. 2018; 26:161–174.
21. Walker G. A review of technologies for sensing contact location on the surface of a display: Review of touch technologies. *J Soc Inf Disp*. 2012; 20:413–440.
22. Barrett, G. Projected-Capacitive Touch Technology. doi:10/gfsjq5
23. Jang Y-S, et al. P-181: A Charge-Share-Based Relative Read-Out Circuit for Capacitance Sensing. SID Symp Dig Tech Pap. 2010; 41:1937–1939.
24. Hamaguchi, M; Nagao, A; Miyamoto, M. 12.3 A 240Hz-reporting-rate 143×81 mutual-capacitance touch-sensing analog front-end IC with 37dB SNR for 1mm-diameter stylus. 2014 IEEE International Solid-State Circuits Conference Digest of Technical Papers (ISSCC); 2014. 214–215. doi:10/gftpsk
25. Jun J, et al. In-Cell Self-Capacitive-Type Mobile Touch System and Embedded Readout Circuit in Display Driver IC. *J Disp Technol*. 2016; 12:1613–1622.
26. An J, Jung S, Hong S, Kwon O. A Highly Noise-Immune Capacitive Touch Sensing System Using an Adaptive Chopper Stabilization Method. *IEEE Sens J*. 2017; 17:803–811.
27. Peumans P, Yakimov A, Forrest SR. Small molecular weight organic thin-film photodetectors and solar cells. *J Appl Phys*. 2003; 93:3693–3723.
28. Cui Y, et al. Over 16% efficiency organic photovoltaic cells enabled by a chlorinated acceptor with increased open-circuit voltages. *Nat Commun*. 2019; 10
29. Tress W, et al. Interpretation and evolution of open-circuit voltage, recombination, ideality factor and subgap defect states during reversible light-soaking and irreversible degradation of perovskite solar cells. *Energy Environ Sci*. 2018; 11:151–165.
30. Huang T-C, et al. Pseudo-CMOS: A Design Style for Low-Cost and Robust Flexible Electronics. *IEEE Trans Electron Devices*. 2011; 58:141–150.
31. CP series lithium manganese primary pouch cells High capacity (5mm), Thin (1 mm) to Ultrathin (0.5 mm) non-rechargeable Lithium Cells from GM Battery and PowerStream. <https://www.powerstream.com/thin-primary-lithium.htm>.

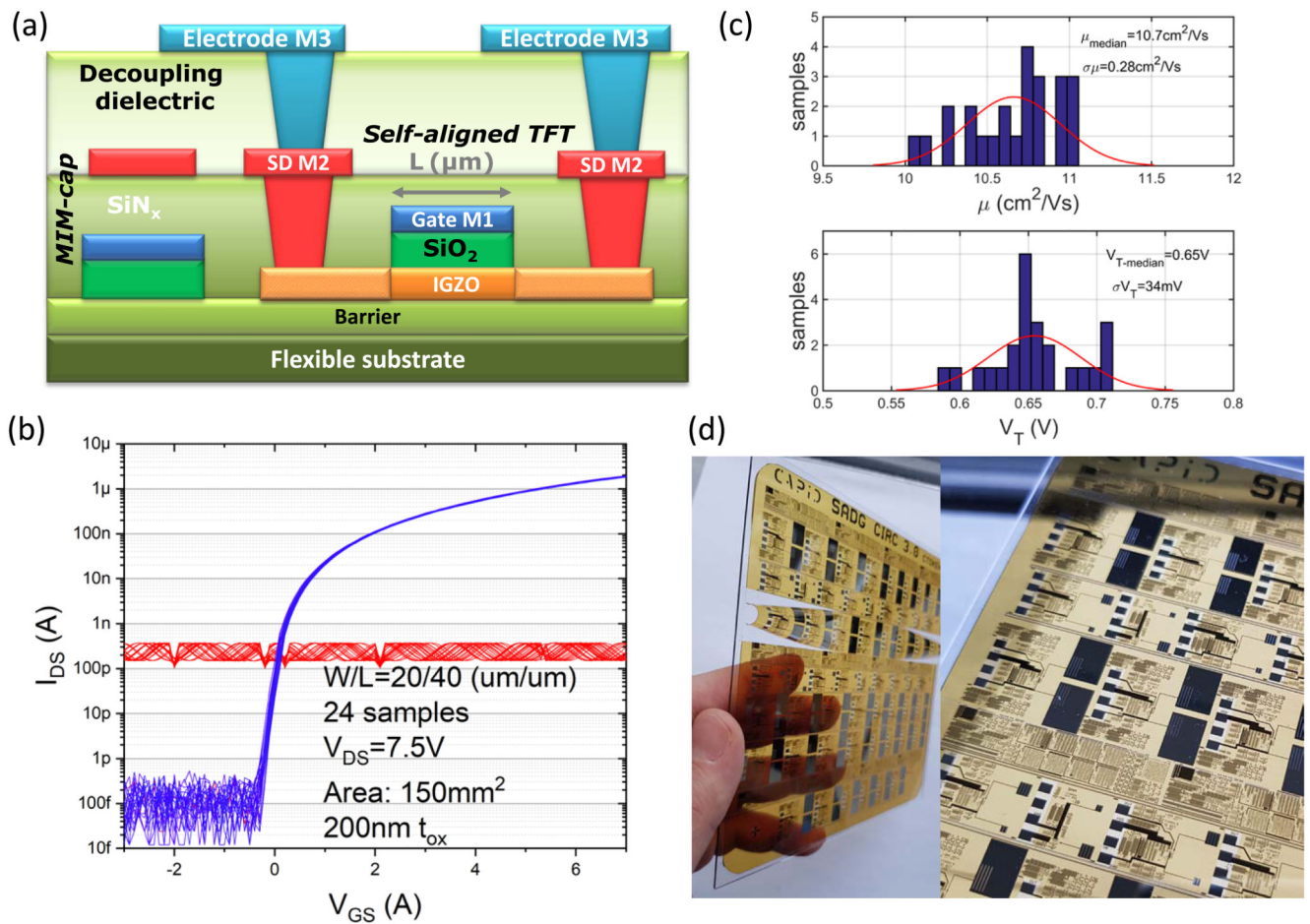


Figure 1. Self-aligned metal-oxide TFT technology.

a,b, Device cross-section **(a)** and TFT transfer curves **(b)** of 24 20 μm/40 μm self-aligned IGZO TFTs on 150 mm² polyimide foil. **c,** Mobility distribution and threshold voltage distribution of various TFTs across a 150mm² wafer. **d,** Photos of the wafers (quarter of a GEN1 plate).

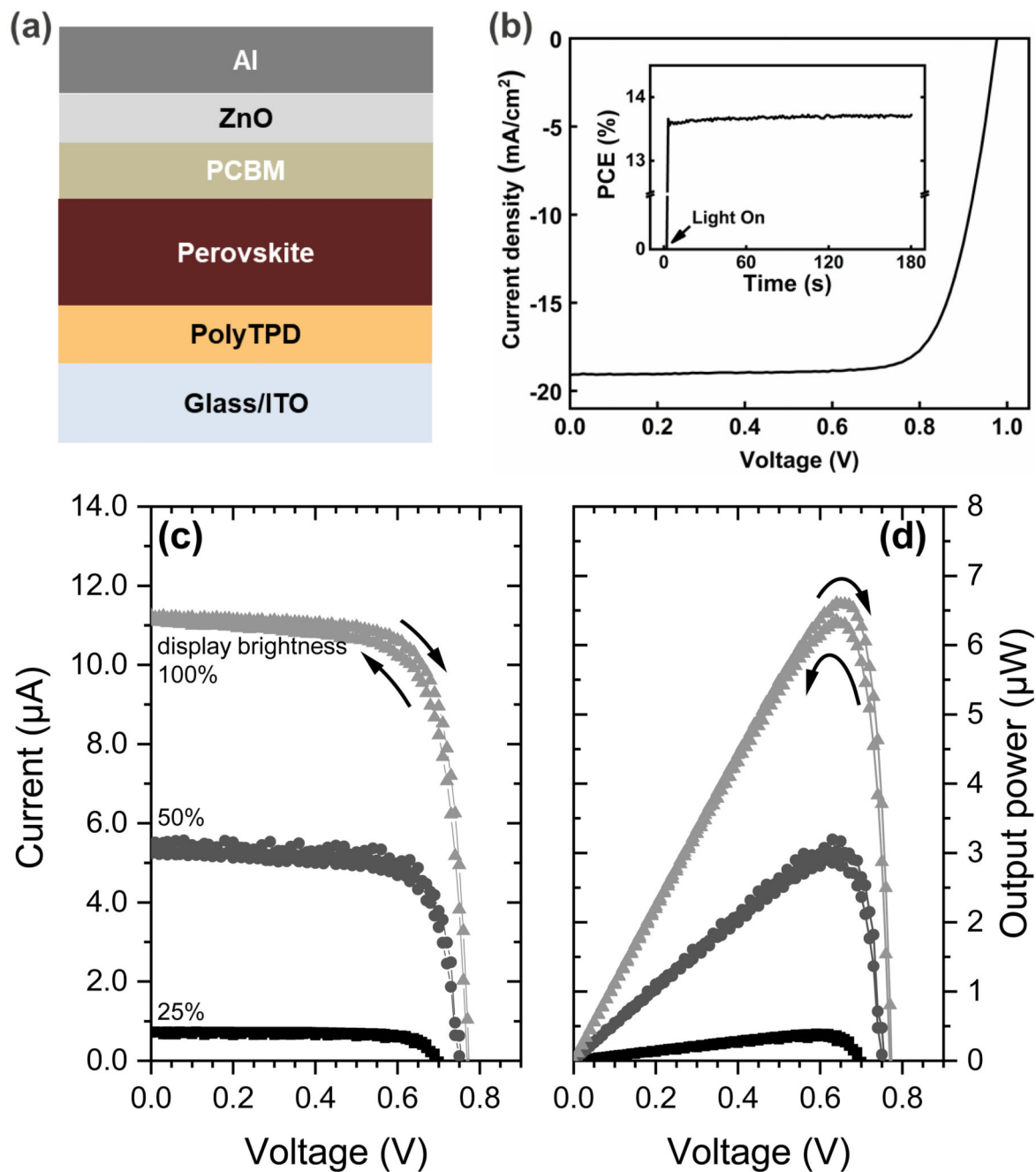


Figure 2. Stack and characterization data of the perovskite solar cells.

a. Schematic of the perovskite solar cell structure. **b.** A typical $J-V$ curve of a single perovskite solar cell measured under AM 1.5G spectrum, with the inset showing the steady PCE when operating at 0.79 V. **c,d.** I-V curve (**c**) and power output (**d**) of one PV cell of 12.5 mm^2 active area placed on a white color screen of a Samsung Galaxy S8 phone.

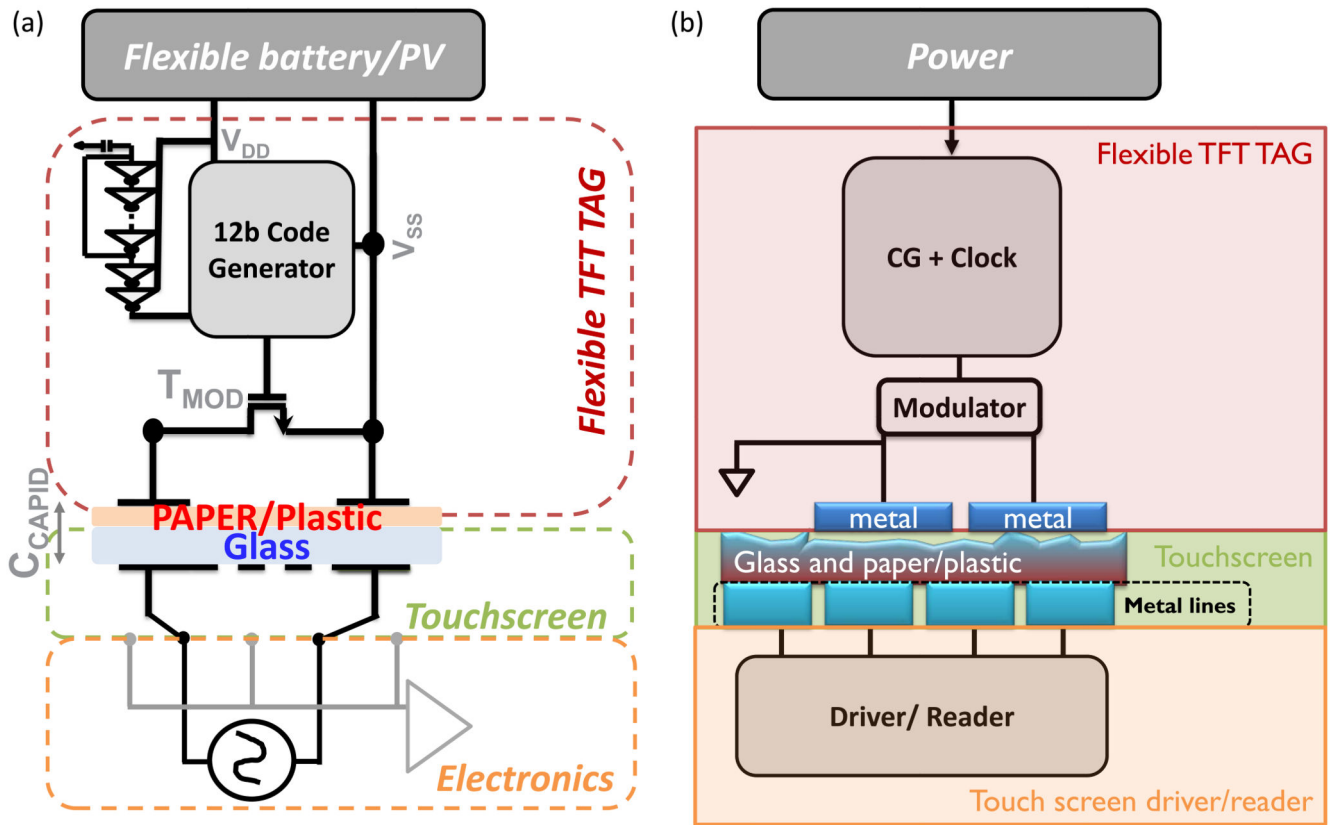


Figure 3. High level C-touch system block diagrams.

a,b, Detailed schematics (a) and system blocks (b) of C-touch tag and touchscreen reader.

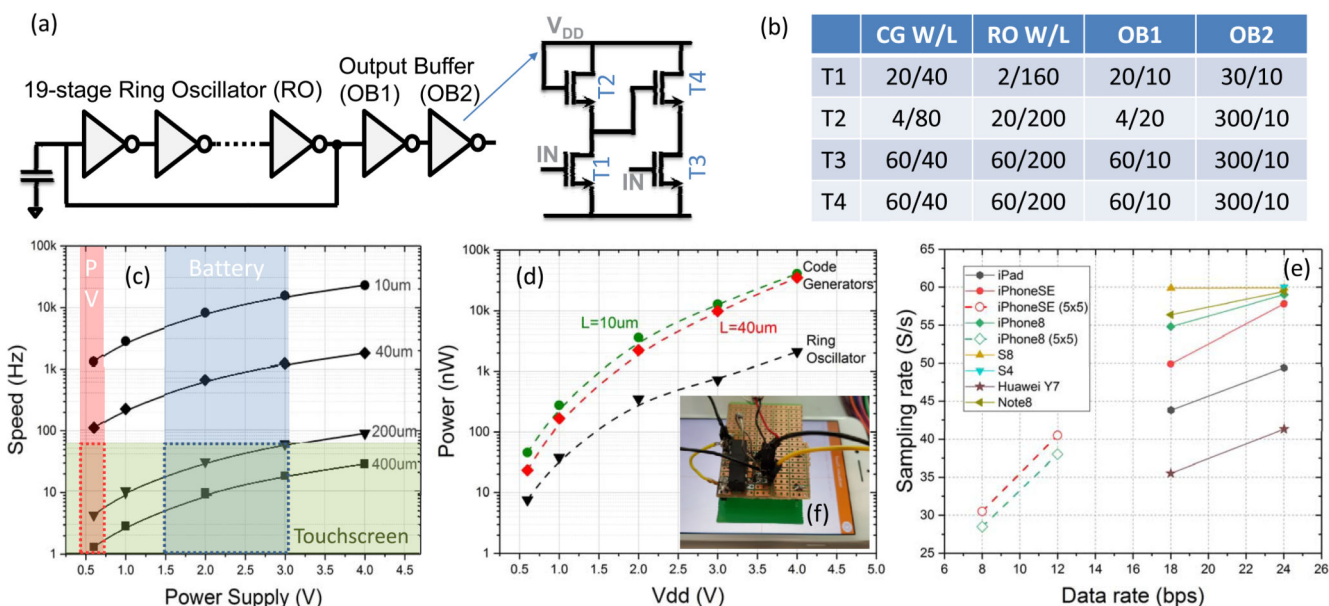


Figure 4. Technical data of the circuit blocks of the c-touch tag.

a. Ring oscillators and inverter gate schematics. **b.** Table comprising TFT sizing of the different blocks. **c.** Speed scaling comparison of four different ring oscillator designs. **d.** Code generator power dissipation measurements data to the applied power supply voltage. **e.** Achieved sampling rate of the touchscreen for various phones and for various electrodes and data rates. **f.** The c-touch emulator built from off-the-shelf silicon parts.

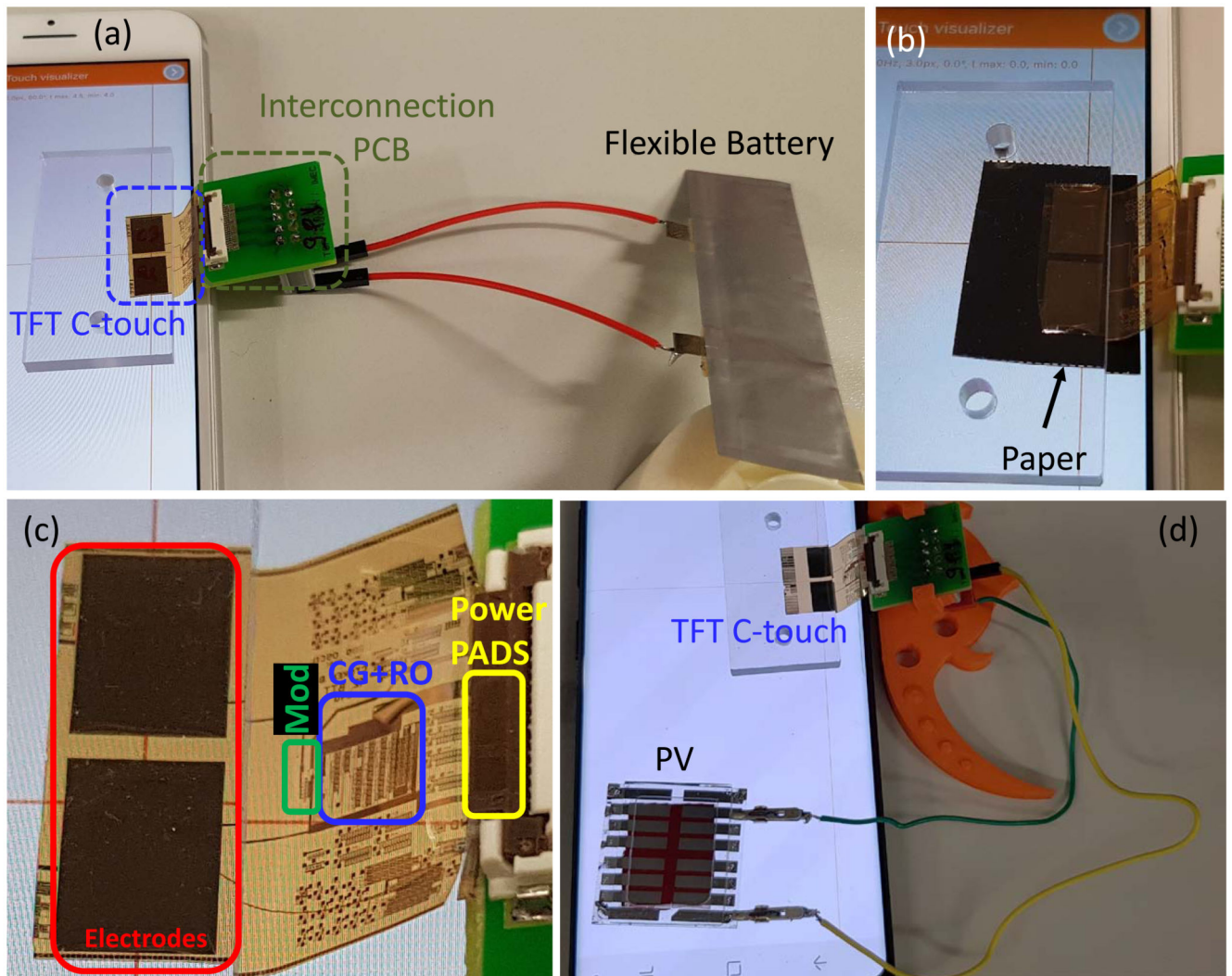


Figure 5. Photos of a flexible touchscreen tag connected to a flexible battery on an iPhone's touchscreen.

a,b, Without (a) and with (b) paper in between. **c,** A zoom-in to the delaminated flexible C-touch tag itself with labels of the various parts. **d,** The C-touch tag powered by a thin-film PV from Samsung S8 display in which only the top-right cell is active.

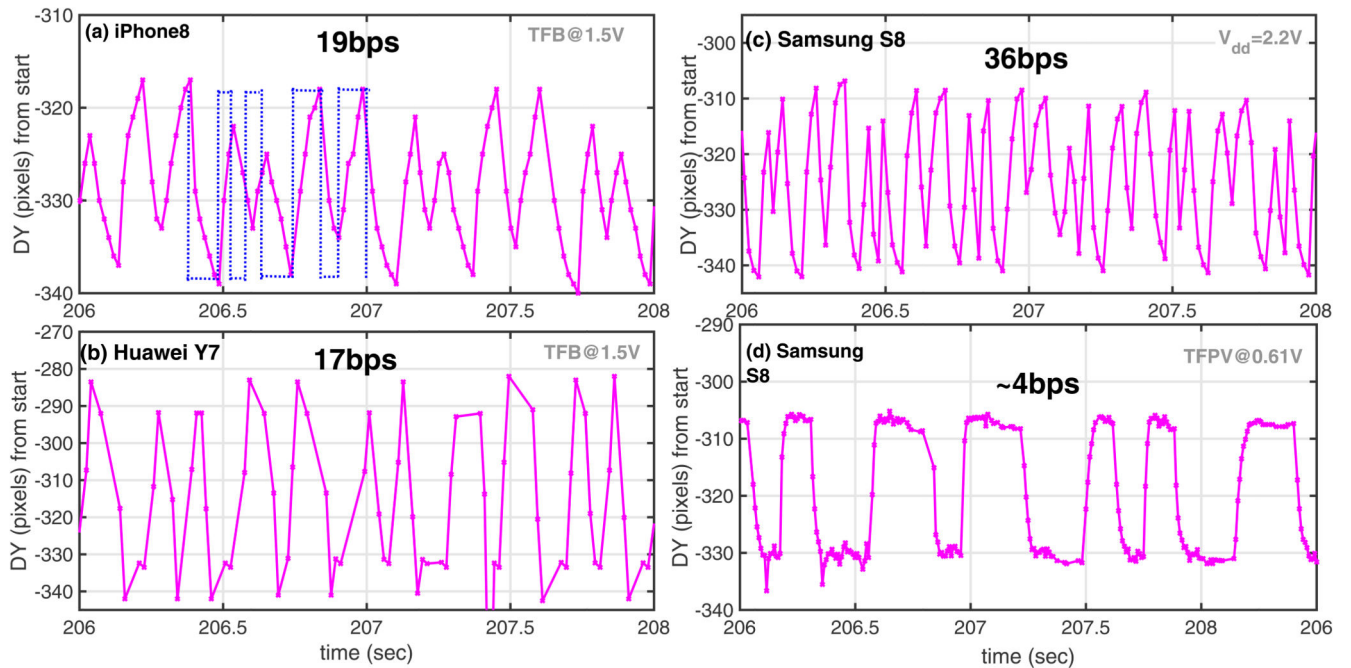


Figure 6. Extracted location data from experiments of C-touch tag performed with various phones.

a, b, Received data on an iPhone 8 (a) and an Huawei Y7 (b), powered by TFB at 1.5V. **c,d,** Received data on Samsung S8 touchscreens powered at 2.2 V (c) and powered by the TFPV at 0.61V (d), which is harvesting the emitted light of the smartphone display.